The Minimally-Invasive Oral Glucose Minimal Model: Estimation of Gastric Retention, Glucose Rate of Appearance, and Insulin Sensitivity From Type 1 Diabetes Data Collected in Real-Life Conditions

Edoardo Faggionato ©, Michele Schiavon ©, Laya Ekhlaspour ©, Bruce A. Buckingham ©, and
Chiara Dalla Man ©

Abstract—Objective: **Modeling the effect of meal composition on glucose excursion would help in designing decision support systems (DSS) for type 1 diabetes (T1D) management. In fact, macronutrients differently affect postprandial gastric retention (GR), rate of appearance (R_a), and insulin sensitivity (S_I). Such variables can be estimated, in inpatient settings, from plasma glucose (G) and insulin (I) data using the Oral glucose Minimal Model (OMM) coupled with a physiological model of glucose transit through the gastrointestinal tract (reference OMM, R-OMM). Here, we present a model able to estimate those quantities in daily-life conditions, using minimally-invasive (MI) technologies, and validate it against the R-OMM.** *Methods:* **Forty-seven individuals with T1D (weight$= 78 \pm 13$ kg, age$= 42 \pm 10$ yr) underwent three 23-hour visits, during which G and I were frequently sampled while wearing continuous glucose monitoring (CGM) and insulin pump (IP). Using a Bayesian Maximum A Posteriori estimator, R-OMM was identified from plasma G and I measurements, and MI-OMM was identified from CGM and IP data.** *Results:* **The MI-OMM fitted the CGM data well and provided precise parameter estimates. GR and R_a model parameters were not significantly different using the MI-OMM and R-OMM ($p > 0.05$) and the correlation between the two S_I was satisfactory ($\rho = 0.77$).** *Conclusion:* **The MI-OMM is usable to estimate GR, R_a, and S_I from data collected in real-life conditions with minimally-invasive technologies.** *Significance:* **Applying MI-OMM to datasets where meal compositions are available will allow modeling the effect of each macronutrient on GR, R_a, and S_I. DSS could finally exploit this information to improve diabetes management.**

***Index Terms*—Bayesian estimation, continuous glucose monitoring, diabetes management, meal composition.**

I. INTRODUCTION

DIABETES mellitus is a metabolic disease characterized by chronic elevated levels of blood glucose (BG) and disorders in the metabolism of carbohydrates, lipids, and proteins. This chronic condition is caused by a deficiency in insulin secretion (type 1 diabetes, T1D), the development of resistance to insulin (type 2 diabetes, T2D), or a combination of the two [1]. Uncontrolled BG levels damage the vascular system and lead to more severe clinical complications over time, including cardiovascular disease, retinopathy, and nephropathy [2]. For this reason, people with diabetes, especially T1D, undergo frequent administration of exogenous insulin analogs to keep BG levels within the safe range (approximately between 70 and 180 mg/dL). However, optimal dosing of this hormone is notoriously a challenging task, due to the presence of several external factors that affect BG levels, such as meals, physical exercise, or psychological stress.

Current T1D therapies involve the administration of an insulin bolus before each meal to anticipate and compensate for the post-prandial glucose excursion. However, current open- and closed-loop control therapies do not take into account meal nutrients different from carbohydrates [3], [4], [5], [6], even if proteins and fats in the meal are known to strongly affect gastric retention (GR, i.e., the fraction of food still in the stomach) [3], [7], glucose rate of appearance (R_a, i.e., the velocity at which glucose is absorbed in the bloodstream) [8], [9], as well as insulin sensitivity (S_I, i.e., the effectiveness of insulin in reducing BG levels) [3], [10]. In turn, all these factors affect the glucose excursion and can lead to a prolonged hyperglycemia if not properly considered in the calculation of the prandial insulin bolus. Therefore, including the information about meal composition in the control algorithms for insulin administration (from the

simplest formulas to the most advanced automatic controllers) would be a significant step toward optimal insulin dosing. Recently, some attempts were made to develop a closed-loop therapy that is able to account for fat intake [11], [12], however, this was achieved by an iterative procedure requiring the patient to undergo several meals with different amounts of fat until a good glycemic target was reached. A more refined approach would be the inclusion of the effect of the meal content directly in the insulin delivery algorithm, however, this step is hampered by the lack of a physiological model quantitatively describing the effect of different macronutrients on BG dynamics. To do this in an effective way, one needs a model able to estimate GR, R_a, and S_I, if possible, in daily-life conditions.

In [13], we proposed a reliable model quantitatively describing glucose traversing through the gastrointestinal tract (esophagus, stomach, intestine), splanchnic bed, and its appearance in the peripheral circulation. However, one needs an R_a profile to identify such a model, which cannot be directly measured but can be estimated, in hospitalized setting, using multiple tracer dilution techniques [14]. Other models were proposed in the literature to estimate R_a after an oral glucose and/or meal challenge (OGTT/MTT), without the need for sophisticated tracer techniques [15], [16]. For instance, the Oral glucose Minimal Model (OMM) [16] allows for simultaneously quantifying both S_I and post-prandial R_a after an OGTT/MTT, assuming a simple piece-wise linear description of the unknown R_a profile. However, parameters describing R_a have not a direct physiological interpretation and, moreover, this method requires plasma glucose and insulin data, thus, it is not usable in free-living conditions. Recently, we incorporated the physiological description of the gastrointestinal tract into the OMM, overcoming the first mentioned limitation of the OMM [17]. Such a modified version of the OMM is still not suitable for our purpose, since it is identified on plasma glucose and insulin data. Nevertheless, here, it was used as the reference method (R-OMM).

To the best of our knowledge, few models [18], [19] tried to describe glucose dynamics in outpatient conditions exploiting data provided by minimally-invasive (MI) devices, i.e., continuous glucose monitoring (CGM) and insulin pump (IP), in subjects with T1D. In both works, the aim was to describe some of the key aspects of glucose regulation in order to evaluate what would have happened if a different insulin dosing was administered. To do that, the authors made some simplifications to the original model structure, especially on the gastrointestinal glucose absorption module, which preclude their use to accurately quantify the key variables characterizing glucose absorption (i.e., GR and R_a). In this work, the aim is to extend the applicability of the R-OMM to outpatient conditions, in subjects with T1D wearing MI devices (i.e., CGM and IP), while also allowing an accurate description of the key processes of gastrointestinal glucose absorption. For such a scope, we resorted to a dataset of real subjects with T1D containing both plasma glucose and insulin measurements, as well as CGM and IP data, after receiving a standardized mixed meal [20]. The simultaneous collection of both plasma glucose and insulin measurements and MI data allowed us to develop the here-called Minimally-Invasive OMM (MI-OMM), identified from MI data, and compare its results in

terms of GR, R_a, and S_I against the R-OMM identified from plasma glucose and insulin data.

II. METHODS

A. Database

The database used in this study is that presented in [20] and is composed of 47 subjects with T1D (age = 42.0 ± 10.1 years, body weight, BW = 77.5 ± 13.4 kg, body mass index, BMI = 24.4 ± 0.1 kg/m^2), recruited in six different clinical centers (Academic Medical Center, Amsterdam, The Netherlands; Centre Hospitalier Regional Universitaire, Montpellier, France; Medical University, Graz, Austria; Profil Institute for Metabolic Research GmbH, Neuss, Germany; University of Cambridge, Cambridge, U.K.; and University of Padova, Padua, Italy) within the AP@home FP7-EU project. The trial was conducted in accordance with the ethics principles set forth in the Declaration of Helsinki and was approved by the medical ethics committees of participating centers (clinical trial reg. no. ISRCTN62034905). Briefly, each subject underwent three randomized 23-hour admissions: one open-loop and two closed-loop sessions. During the open-loop admission, subjects were treated with their usual insulin therapy through an IP whereas, during the closed-loop admissions, two different control algorithms were used for insulin infusion. Subjects received a mixed meal for dinner (19:00, first day), breakfast (08:00, second day), and lunch (12:00, second day) containing 80 g, 50 g, and 60 g of carbohydrates and standardized macronutrient composition, respectively, and performed 30 minutes of moderate physical activity (15:00, second day). In case of hypoglycemia, subjects were treated with 15 g carbohydrate snacks until the recovery to normal glucose levels. Blood samples were collected to measure plasma glucose and insulin every 15 min in the first 2 hours after a meal and during physical activity, every hour during bedtime (from 23:00, first day, to 7:00, second day), and every 30 min in the rest of the admission.

Plasma glucose (Fig. 1, panel A) was measured using YSI 2300STAT Plus Analyzer (YSI Incorporated, Yellow Springs, OH, USA) and plasma insulin (Fig. 1, panel B) was measured using an insulin chemiluminescence assay (Invitron Ltd, Monmouth, U.K.). Throughout the admissions, subjects wore a CGM system (Dexcom Seven Plus CGM, Dexcom, San Diego, CA) which collected glucose measurements every 5 minutes (Fig. 1, panel C), and an insulin patch-pump (Omnipod, Insulet, Bedford, MA) which administered insulin every 5 minutes (Fig. 1, panel D). Calibration of the sensor was performed using fingerstick glucose measurements (self-monitoring of blood glucose, SMBG) before dinner (18:75, first day), before bedtime (23:00, first day), before breakfast (07:00, second day) and before the exercise session (14:50, second day), as per manufacturer's instructions. More information about the protocol is reported in [20].

For the purpose of this work, only data from 15 minutes before (06:45 pm) to 8 hours after dinner (03:00 am) were considered to avoid the need to model the so-called "dawn phenomenon", usually occurring from 03:00 to 07:00 [21]. From the 141 available sessions, 16 were discarded due to problems in insulin administration (pump replacement, pump occlusion, or missing
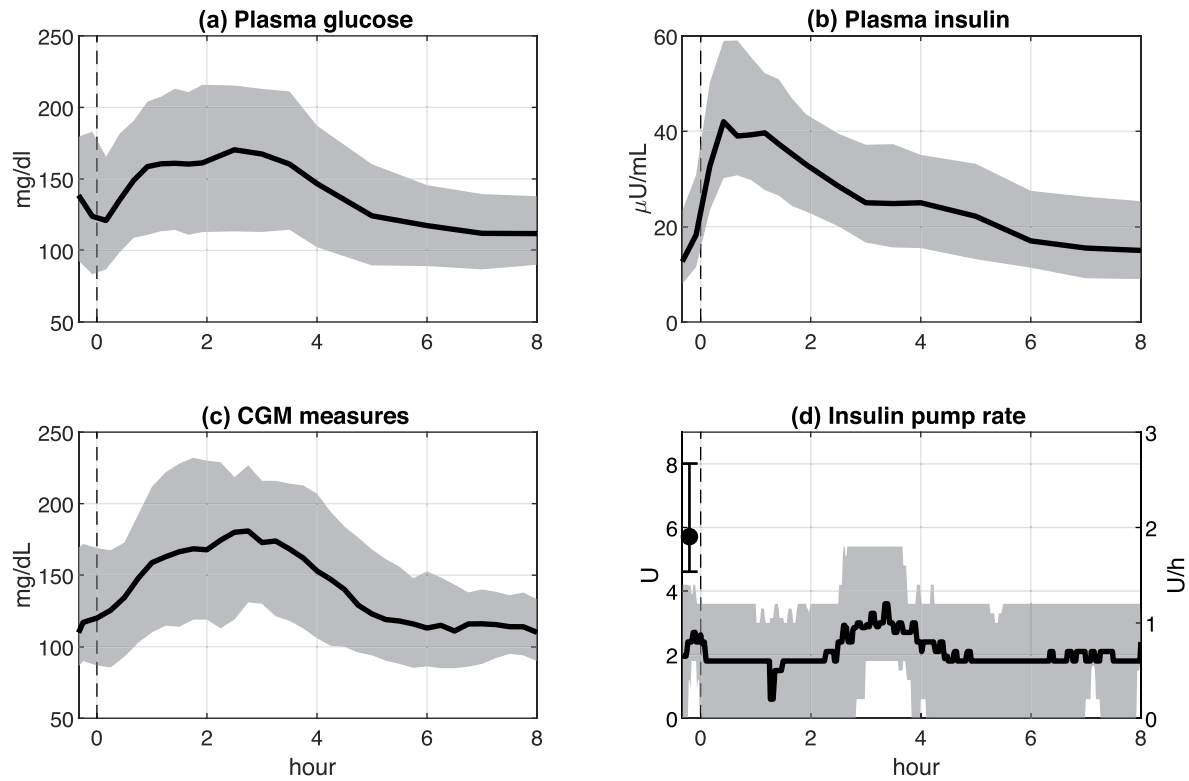
Fig. 1. Median (solid black lines) and 25th and 75th percentiles (gray shaded area) of the data used for model development and validation. *Panel A:* plasma glucose concentration. Dashed lines represent mealtime. *Panel B:* plasma insulin concentration. *Panel C:* CGM sensor measurements. *Panel D:* Insulin pump rate (right y-axis, solid line and shaded areas) and pre-prandial insulin bolus (left y-axis, dot and bars). The black dot represents the median pre-prandial bolus while the lower and upper bars represent the 25th and 75th percentiles, respectively. All the plots are aligned with mealtime at 19:00 on the first day (0 hours).
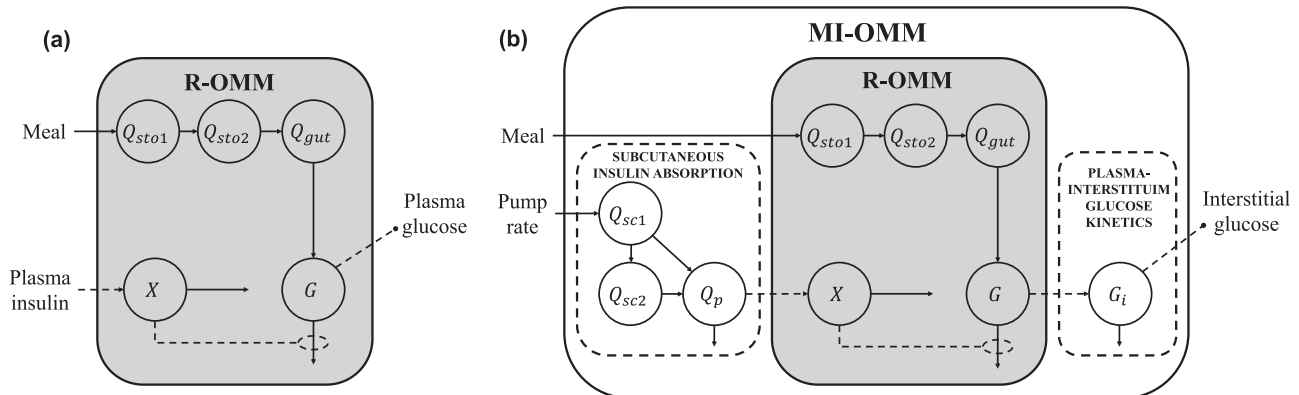

Fig. 2. Schematic representation of the models used in this work. *Panel A:* Reference oral minimal model (R-OMM) used in [17]. *Panel B:* Minimally-invasive oral minimal model (MI-OMM) developed in this work, which integrates the R-OMM, a model of subcutaneous insulin absorption, and a model of plasma-interstitium glucose kinetics. Circles represent state variables, continuous arrows represent mass transfers and inputs, and dashed lines represent controls. Dashed lines with black dots represent the measurement variables.

bolus), and 8 due to missing or erroneous CGM sensor data. Therefore, a total of 117 sessions of 8 hours were used for model development and validation. In Fig. 1, median and interquartile range (25th and 75th percentiles) of such data are reported.

B. The Reference Oral Glucose Minimal Model (R-OMM)

This model originated from the OMM [16] which describes plasma glucose dynamics after a meal as a function of the measured plasma insulin concentration and the unknown meal glucose R_a. However, at variance with [16], where R_a was approximated by a piece-wise linear function with fixed breakpoints and amplitudes to be estimated from the data, here, we used the structural model of the gastrointestinal tract proposed in [13] which provides meaningful parameters describing the physiology of the gastrointestinal tract (Fig. 2, panel A). This revisited version of the model was already used as a reference

model in other modeling studies [17]. Model equations are:

$$
\begin{cases}
\dot{G}(t) = -[p_1 + X(t)]G(t) + p_1 G_b + \frac{R_a(t)}{V_G} & G(0) = G_0 \\
\dot{X}(t) = -p_2 X(t) + p_2 S_I[I_p(t) - I_b] & X(0) = X_0
\end{cases} \quad (1)
$$

where $G(t)$ is plasma glucose, $X(t)$ is insulin action in a remote compartment, and $I_p(t)$ is the plasma insulin concentration, G_b and I_b are basal levels of glucose and insulin in plasma, V_G is the volume of glucose distribution, p_1 is the fractional glucose effectiveness, p_2 is the rate constant describing the dynamics of insulin action, and S_I is insulin sensitivity, i.e., the ability of insulin to suppress glucose production and enhance glucose utilization. $R_a(t)$ is the post-prandial glucose rate of appearance in plasma and is described by the following differential equations [13], whose parameters and variables have a straightforward and clear physiological interpretation:

$$
\begin{cases}
\dot{Q}_{sto1}(t) = -k_{max}Q_{sto1}(t) + D\delta(t) & Q_{sto1}(0) = 0 \\
\dot{Q}_{sto2}(t) = -k_{empt}(t)Q_{sto2}(t) + k_{max}Q_{sto1}(t) & Q_{sto2}(0) = 0 \\
\dot{Q}_{gut}(t) = -k_{abs}Q_{gut}(t) + k_{empt}(t)Q_{sto2}(t) & Q_{gut}(0) = 0 \\
R_a(t) = \frac{f}{BW}k_{abs}Q_{gut}(t)
\end{cases}
$$
$$(2)$$

where D is the amount of ingested glucose, $Q_{sto1}(t)$ and $Q_{sto2}(t)$ represent the amount of glucose in the stomach (solid and liquid phase, respectively), and $Q_{gut}(t)$ is the amount of glucose in the intestine. k_{max} is the constant rate of meal grinding, k_{abs} the constant rate of intestinal absorption, f is the fraction of glucose that is actually absorbed in plasma (i.e., glucose bioavailability), and BW is the body weight of the subject. $k_{empt}(t)$ represents the rate of gastric emptying, which varies depending on the total amount of glucose in the stomach $Q_{sto}(t) = Q_{sto1}(t) + Q_{sto2}(t)$, according to the formula:

$$
k_{empt}(t) = k_{min} + \frac{k_{max} - k_{min}}{2}\Big\{\tanh[\alpha(Q_{sto}(t) - cD)]
$$
$$
- \tanh[\beta(Q_{sto}(t) - dD)] + 2\Big\} \quad (3)
$$

with $\alpha = 5/[2D(1-c)]$ and $\beta = 5/(2Dd)$, and c and d the model parameters that determine the flex points of the curve describing the behavior of k_{empt} as function of Q_{sto}, with k_{min} and k_{max} the minimal and maximal constant rates of stomach emptying. For a complete description of (3), we refer to the original work [13].

C. The Minimally-Invasive Oral Glucose Minimal Model (MI-OMM)

The MI-OMM model couples the R-OMM described in (1)–(3), with the descriptions of subcutaneous absorption of fast-acting insulin analogues [22], [23] (Section II-C1), and plasma-interstitium glucose kinetics [24], [25] (Section II-C2) (Fig. 2, panel B). The incorporation of these modules extended the usability of the R-OMM to non-hospitalized experimental settings since it allowed describing CGM data as a function of subcutaneous insulin infusion rate and the ingested amount of carbohydrates while keeping the model's ability to provide parameters and variables with a clear physiological meaning.

1) Subcutaneous Insulin Absorption and Plasma Insulin Kinetic Model:
The subcutaneous insulin absorption model [22], [23], coupled with a single-compartment model of insulin kinetics in plasma [26], is described by the following differential equations:

$$
\begin{cases}
\dot{Q}_{sc1}(t) = -(k_{a1}+k_d)Q_{sc1}(t) + U(t-\tau_I) & Q_{sc1}(0) = Q_{sc1,0} \\
\dot{Q}_{sc2}(t) = -k_{a2}Q_{sc2}(t) + k_d Q_{sc1}(t) & Q_{sc2}(0) = Q_{sc2,0} \\
\dot{Q}_p(t) = -k_e Q_p(t) + k_{a1}Q_{sc1}(t) \\
\qquad\qquad + k_{a2}Q_{sc2}(t) & Q_p(0) = Q_{p,0} \\
I_p(t) = \frac{Q_p(t)}{V_I}
\end{cases}
$$
$$(4)$$

where $U(t)$ is the pump rate infusion, $Q_{sc1}(t)$ and $Q_{sc2}(t)$ represent the amount of insulin in the subcutis (non-monomeric and monomeric state, respectively), $Q_p(t)$ and $I_p(t)$ are the insulin amount and concentration in plasma, respectively. k_{a1} and k_{a2} are the constant rate of insulin absorption in plasma from the two subcutaneous compartments, k_d is the constant rate of insulin dissociation in monomers, k_e is the constant fractional insulin clearance in plasma, and V_I is the plasma insulin distribution volume.

2) Interstitial Glucose Kinetic Model:
The diffusion process of glucose from the blood, $G(t)$, to the interstitial space, $G_i(t)$, is modeled by a linear single-compartment model, corrected for the plasma-to-interstitium glucose gradient in steady-state conditions, as reported in [24], [25]:

$$
\dot{G}_i(t) = -\frac{1}{\tau_G}G_i(t) + \frac{1}{\tau_G}G(t) \qquad G_i(0) = G_{i,0} \quad (5)
$$

where $G_i(t)$ is interstitial glucose concentration and τ_G is the equilibration time constant between plasma and interstitium.

D. Model Identification

1) R-OMM Identification:
The R-OMM is *a priori* nonidentifiable, i.e., an infinite number of solutions for model parameters exists [27]. In particular, paralleling what was done in [16] and [17], we fixed $V_G = 1.45$ dL/kg and, to help numerical identifiability, $f = 0.9$. In addition, to avoid nonphysiological parameter configurations we constrained k_{max} to be greater than k_{min} and c to be greater than d, as done in [13]. Finally, as done in [25] and [17], p_1 was reparametrized to separate the insulin-dependent and -independent components that both contribute to the fractional glucose effectiveness [28]:

$$
p_1 = \frac{GEZI}{V_G} + S_I I_b \quad (6)
$$

where I_b was obtained from the plasma insulin data at the end of the meal session. Therefore, the final set of model parameters of the R-OMM to be estimated was S_I, p_2, G_b, GEZI, k_{abs}, k_{max}, k_{min}, c, and d.

R-OMM was numerically identified on plasma glucose data using the amount of carbohydrate ingested as input and plasma insulin concentration as model *forcing-function*, hence assumed to be known without error. Model parameters were estimated using a Bayesian Maximum A Posteriori estimator [29], using prior information coming from the literature [16], [30]. Measurement error on glucose data was assumed to be independent,

Gaussian, with zero mean and known standard deviation (constant coefficient of variation, CV=2%).

2) MI-OMM Identification: The MI-OMM is *a priori* non-identifiable. In particular, we fixed: V_I=0.135 L/kg and, as for the R-OMM, V_G=1.45 dL/kg, and f=0.9. In addition, to help numerical identifiability, we fixed to population values τ_I=5.62 min, $k_{a1} = 1.34 \cdot 10^{-4}$ min^{-1}, $k_d = k_{a2} + 0.0155$ min^{-1} [23], and the same constraints to parameter k_{max} and k_{min}, c, and d were imposed as for the R-OMM. Parameter p_1 was reparametrized as reported in (6). In addition, here we calculated I_b from pump data as

$$I_b = \frac{U_b}{k_e\,V_I\,BW} \tag{7}$$

where Ub is the basal insulin infusion rate of the subject in the last hour before the start of the experiment. Hence, the final set of model parameters of the MI-OMM to be estimated was S_I, p_2, G_b, GEZI, k_{abs}, k_{max}, k_{min}, c, d, k_{a2}, k_e, and τ_G. MI-OMM was identified simultaneously on CGM sensor and, if available, SMBG data using the amount of the ingested carbohydrate and the subcutaneously administered exogenous insulin profile as model inputs. As known from literature [31], CGM traces of old-generation sensors (like the Dexcom Seven Plus used here) were affected by temporal and proportional drift and offset. These were accounted in the model by modulating $G_i(t)$ of (5) as follows:

$$CGM(t) = (a_0 + a_1 t)\,G_i(t) + b_0 + b_1 t \tag{8}$$

where a_0, a_1, b_0, and b_1 are the parameters describing the offset (subscript 0) and the temporal drift (subscript 1) of the sensor after a sensor calibration, to be estimated from the data in each between-calibration interval. Of note, on some occasions, the confidence interval of the estimated parameters of the CGM error model may include the zero term. In this case, the CGM error model can be simplified by fixing these values to zero. Moreover, the noise superimposed to CGM, $v(t)$, is known to be colored. To account for that, we used the autoregressive model of order 2 reported in [31]. Needless to say, the choice of the appropriate CGM model depends upon the CGM device used in the experiment. For instance, in more recent CGM devices, drift and offset might be negligible and the superimposed error noise could be described by a simpler model. Measurements noise on SMBG data, $w(t)$, was assumed to be independent, Gaussian with constant CV=2%. To facilitate the *a posteriori* identifiability, model parameters were estimated using a Bayesian Maximum A Posteriori estimator [29], with the *a priori* probability density function assumed to be log-normally distributed, with known mean μ_p and covariance matrix Σ_p of the log-transformed parameters, derived from the literature [16], [23], [30], [31]. In summary, the objective function to minimize was:

$$J(\hat{\theta}) = \hat{v}^T\Sigma_v^{-1}\hat{v} + \hat{w}^T\Sigma_w^{-1}\hat{w} + (\hat{\theta} - \mu_p)^T\Sigma_p^{-1}(\hat{\theta} - \mu_p) \tag{9}$$

where $\hat{v}$ is the difference between measured and predicted CGM, Σ_v the covariance matrix of $v(t)$, calculated from the autoregressive model proposed by Facchinetti and coworkers [31] using the Yule-Walker's equation [32], $\hat{w}$ is the difference between

measured SMBG and model predicted glucose concentration, Σ_w the covariance matrix of $w(t)$, and $\hat{\theta}$ is the estimated vector of the log-transformed parameters.

Model identification was performed in MATLAB (MATLAB R2020a, The MathWorks, Inc., Natick, Massachusetts, United States [33]) using the `ode45()` solver to integrate differential equations and the `lsqnonlin()` built-in function to find model parameters minimizing (9).

E. Model Assessment and Validation

The model assessment was performed by checking for randomness and normality distribution of weighted residuals, *a posteriori* identifiability, and physiological plausibility of parameter estimates [29]. Randomness of weighted residuals was assessed by the Runs test and normality of the distributions by the Kolmogorov-Smirnov test. Precision of parameter estimates was expressed as percentage CV for those that can assume only positive values and as standard deviation (SD) otherwise. In both cases, SD was derived from the square root of the diagonal elements of the covariance matrix of the estimates, which, in turn, was obtained as the inverse of the Fisher Information matrix. Physiological plausibility of model parameters was assessed by checking if the value of the estimates falls inside a physiological range.

MI-OMM validation was performed by comparing key clinically relevant quantities, i.e., S_I, $R_a(t)$, and GR(t) calculated as:

$$GR(t) = 100\,\frac{Q_{sto}(t)}{D} \tag{10}$$

derived from the MI-OMM, against those obtained from the reference R-OMM. Finally, MI-OMM prediction of plasma glucose and insulin profiles were visually compared against the measured plasma glucose and insulin concentration that were available in the dataset but not used in the identification process.

F. Statistical Analysis

Data and results are reported as median and interquartile range (25th, 75th percentile) unless otherwise specified. Two-sample comparisons were done by Student's T-test, for normally distributed variables, Wilcoxon's signed rank test, otherwise. Pearson's correlation was used to evaluate univariate linear correlation, in the case of normally distributed variables, or Spearman's ranked correlation, otherwise. Normality of the parameter distributions was assessed by the Lilliefors' test.

III. RESULTS

A. Model Assessment

The R-OMM predicted plasma glucose data well both in the overall population and at a single individual level and provided precise estimates of model parameters (not shown).

The MI-OMM was able to satisfactorily predict CGM data both in the overall population and at a single individual level. Mean and standard deviation of weighted residuals over time are reported in Fig. 3. They were reasonably uncorrelated with
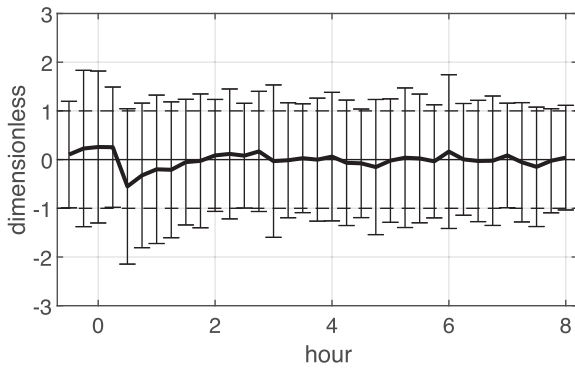
Fig. 3.   Average weighted residuals of the model (black solid line); vertical bars represent $\pm$ one standard deviation.
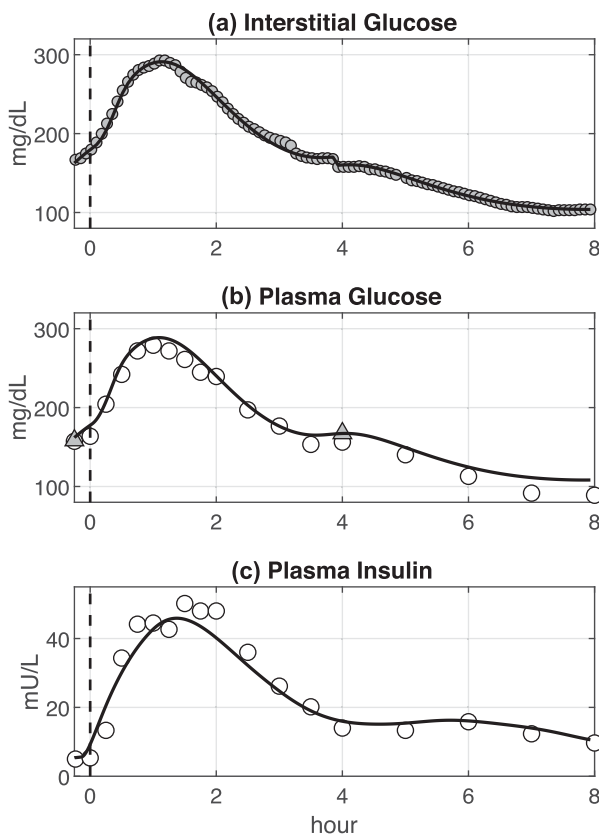

Fig. 4.   MI-OMM predicted signals for a representative subject. *Panel A:* Model predicted CGM (thick black line) plotted against CGM data (grey dots). *Panel B:* Model predicted G(t) (thick black line) plotted against plasma glucose data (white dots) and SMBG measurements (grey triangles). *Panel C:* Model predicted I(t) (black thick line) plotted against plasma insulin data (white dots). Dashed vertical lines at time zero indicate mealtime.

approximately unitary variance. The CGM signal predicted by the MI-OMM and the measured CGM data are shown for a representative subject in panel A of Fig. 4.

As an independent validation, plasma insulin and glucose concentration data predicted by MI-OMM (despite such data were not used for model identification) well compared with their measured counterparts, as it can be seen in panels B and C of Fig. 4,

for the same representative subject. Estimated model parameters are reported in Table I, together with the mean CV, proving the ability of the model to estimate physiologically plausible parameters with precision. The only parameter estimated with poor precision was k_{abs}, for which we found CV between 100% and 112% in 7 out of 117 sessions. Estimated error parameters are reported in Table II. They showed distributions comparable to those reported in the original work. Their precision is expressed as SD because the CV is not suitable for this type of variable that can assume both positive and negative values.

B. Model Validation

The comparison of the MI-OMM with the R-OMM provided satisfactory results. In particular, Spearman's ranked correlation between S_I estimated with the two models was 0.77 (p<0.01). In addition, the probability density functions of the S_I estimated with the two models were not statistically different (p=0.33). The visual comparison of the two distributions is shown in panel A of Fig. 5, while a point-to-point comparison is shown in panel B of the same figure.

Moreover, the MI-OMM provided GR(t) and $R_a(t)$ curves similar to those obtained with the R-OMM, as it can be seen in panels A and B of Fig. 6, where their medians and 25th and 75th percentiles are reported. The model predicted also plasma glucose well while overestimating plasma insulin peaks, as shown in panels C and D of Fig. 6.

Finally, also the probability density functions of all the parameters related to the glucose absorption (i.e., k_{abs}, k_{max}, k_{min}, c, and d) estimated with the two models were not statistically different (p>0.05).

IV. DISCUSSION

The performance of both decision support systems for diabetes management and artificial pancreas algorithms would benefit from the knowledge of how and how much non-carbohydrates macronutrients alter post-prandial gastric retention and glucose absorption [5]. A few studies were performed in hospitalized settings, e.g., [6], [34], however, now that large CGM data sets collected in free-living conditions are available, it would be useful to have a tool to accurately estimate such key variables in these experimental conditions from such minimally-invasive devices.

In this work, we developed a semi-mechanistic model that provides an accurate description of gastric retention, glucose rate of appearance, and insulin sensitivity in patients with T1D wearing a CGM sensor and an IP. We focused our attention on those three quantities since they are known to be highly affected by different meal compositions [5] and developed a model to assess those variables, as accurately as possible, in real-life conditions.

To do that, we started from a modified version of the validated OMM [16], incorporating a semi-mechanistic model of glucose transit through the gastrointestinal tract [13] and able to describe GR, R_a and S_I in hospitalized patients, using plasma glucose and insulin measurements. Such a model was also used as a reference (R-OMM) to assess the performance of the proposed

TABLE I
ESTIMATED MODEL PARAMETERS

Parameter	Unit	25th percentile	50th percentile	75th percentile	mean CV
S_I	$\frac{1}{\mu U/mL \cdot min}$	$3.64 \cdot 10^{-4}$	$5.50 \cdot 10^{-4}$	0.00109	41%
k_{abs}	min^{-1}	0.0253	0.0496	0.139	68%
k_{max}	min^{-1}	0.0235	0.0295	0.0355	39%
k_{min}	min^{-1}	0.00622	0.00807	0.0101	23%
c	dimensionless	0.760	0.872	0.923	41%
d	dimensionless	0.218	0.283	0.347	12%
p_2	min^{-1}	0.00984	0.0103	0.0116	19%
G_b	mg/dL	102	117	129	12%
GEZI	$\frac{1}{kg/dL \cdot min}$	0.00967	0.0100	0.0103	19%
τ_G	min	5.58	7.76	12.3	34%
k_{a2}	min^{-1}	0.0109	0.0129	0.0164	27%
k_e	min^{-1}	0.109	0.116	0.126	30%

Twenty-fifth, 50th, and 75th percentiles of the estimated model parameters, and their precision expressed as mean percentage coefficient of variation (CV).

TABLE II
ESTIMATED ERROR PARAMETERS

Parameter	Unit	25th percentile	50th percentile	75th percentile	mean SD
a_0	dimensionless	0.929	1.01	1.19	0.118
a_1	min^{-1}	$-7.35 \cdot 10^{-4}$	$-4.6 \cdot 10^{-4}$	$4.55 \cdot 10^{-4}$	$6.36 \cdot 10^{-4}$
b_0	$\frac{mg}{dL}$	-48.4	-26.5	21.9	24.5
b_1	$\frac{mg}{dL \cdot min}$	-0.046	0.0784	0.117	0.0834

Twenty-fifth, 50th, and 75th percentiles of the estimated model parameters, and their precision expressed as mean standard deviation (SD).

MI-OMM, which extends the domain of validity of the R-OMM to work in outpatient conditions, using data coming from MI devices.

We proved that MI-OMM can satisfactorily fit the CGM profiles and generally provide precise and physiologically reliable parameter estimates. The only exception was parameter k_{abs}, which was estimated with poor precision ($100\% < CV < 112\%$) in 7 out 117 analyzed sessions. This was imputable to the weak *a priori* information associated with that parameter, which in fact presented the highest *a priori* variance overall, with $CV = 168\%$. A further validation of the model was the comparison of plasma glucose and insulin prediction against the measured concentration. Plasma glucose concentration was predicted well, while plasma insulin concentration was predicted with kinetics that appear faster than the observed ones, thus, leading to the overestimation of the insulin peaks. This was probably due to the employed prior distributions for k_{a2} and k_e, which were derived from a model developed on data coming from a single insulin injection in hospitalized patients and, therefore, that may present different kinetics than those shown in this case. However, this does not seem to affect the quantities of interest, such as S_I, probably due to compensation with the parameter p_2. Overall model performance is still acceptable even if prior information was not perfectly adequate for insulin kinetics parameters. This is likely the result of the robust physiology-based model structure and the availability of an informative prior for the remaining parameters, both contributing to the *a posteriori* identifiability of this complex model and maintaining its physiological interpretability.

The most important feature of the MI-OMM is that it provides estimates of GR, R_a, and S_I that well matched their R-OMM counterparts, both in terms of correlation, median, and variability. The same result holds for all the model parameters related to the gastrointestinal tract, like minimal (k_{min}) and maximal (k_{max}) gastric emptying and gut absorption (k_{abs}). Further studies are needed to assess if some, all, or none of these parameters/curves are good predictors of meal composition, but we foresee that meals with high relative fat content should present slower GR and R_a profiles. To quantitatively characterize these two curves one could compute indices like the half-life of the GR curve [35], and the area under the R_a profile in the first 2 hours after the meal [36], normalized to the amount of ingested carbohydrates. We found that also the distribution of these two indices estimated from MI-OMM-derived curves well matched their R-OMM-derived counterparts (not shown).

A first limitation of the presented work is that all the patients received a mixed meal of 60 g of carbohydrates and standardized macronutrient composition during the experiment. Therefore, the variability observed in model parameters/curves is likely to be underestimated compared to those one would find in real-life conditions, where meals with different compositions are consumed. This is a drawback of the dataset, which however presented an important and unique feature, i.e., the frequent collection of both plasma measurements and CGM data. Preliminary results obtained on an independent dataset of subjects with T1D, studied in real-life conditions while wearing CGM and IP, showed promising results in terms of model ability to detect differences between high-fat and low-fat meals [37].
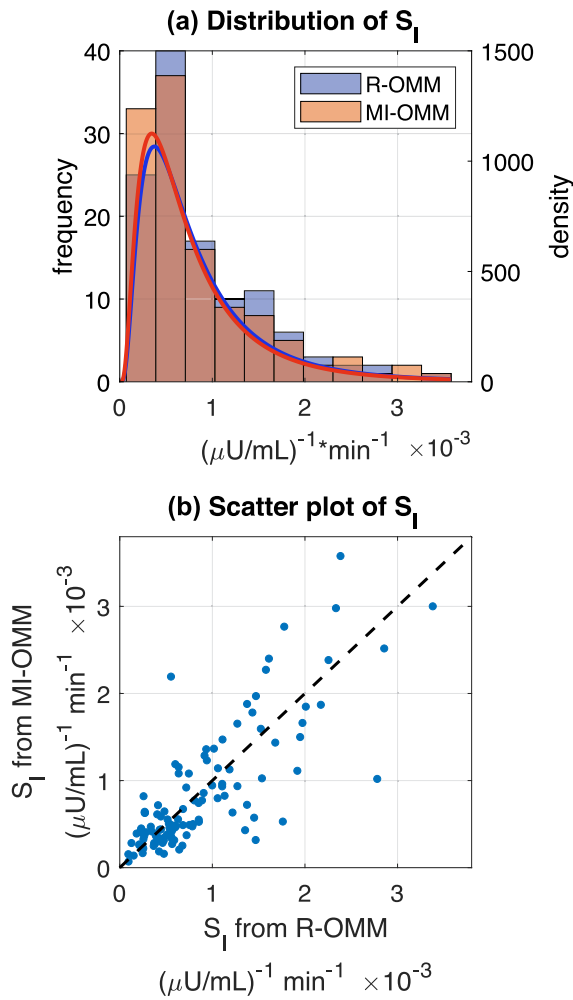
Fig. 5. Comparison between the S_I estimated with the two models. *Panel A:* Comparison between histograms (left y-axis) and probability density functions (right y-axis). Light blue and orange bars represent the frequency of S_I estimated with the R-OMM and the MI-OMM, respectively. Blue and red thick lines represent the log-normal distribution curves fitted against S_I obtained with the R-OMM and the MI-OMM, respectively. *Panel B:* Point-to-point comparison of S_I estimated with the R-OMM and the MI-OMM. The dashed black line is the bisector of the first quadrant.

A second limitation is that the assumptions for the calculation of the initial conditions of the model (see Appendix A) might have hampered the fit of the data in the first minutes, affecting the estimate precision. For example, the slight undershoot in the pattern of the residuals in the first hour (see Fig. 3) might be caused by an inaccurate model initialization in some sessions. This could have led to an imprecise estimation of the parameter k_{abs} whose estimation strongly relies on the measurements immediately after the meal, which are directly related to the rapid carbohydrate absorption. However, this problem would be reasonably overcome if the model was incorporated in a control algorithm working online, or ensuring that the patient is in a reasonable steady state prior to starting the experiment.

A final remark is that the dataset of the present study was collected using an outdated CGM sensor (Dexcom Seven Plus CGM, Dexcom, San Diego, CA). With this in mind, we can
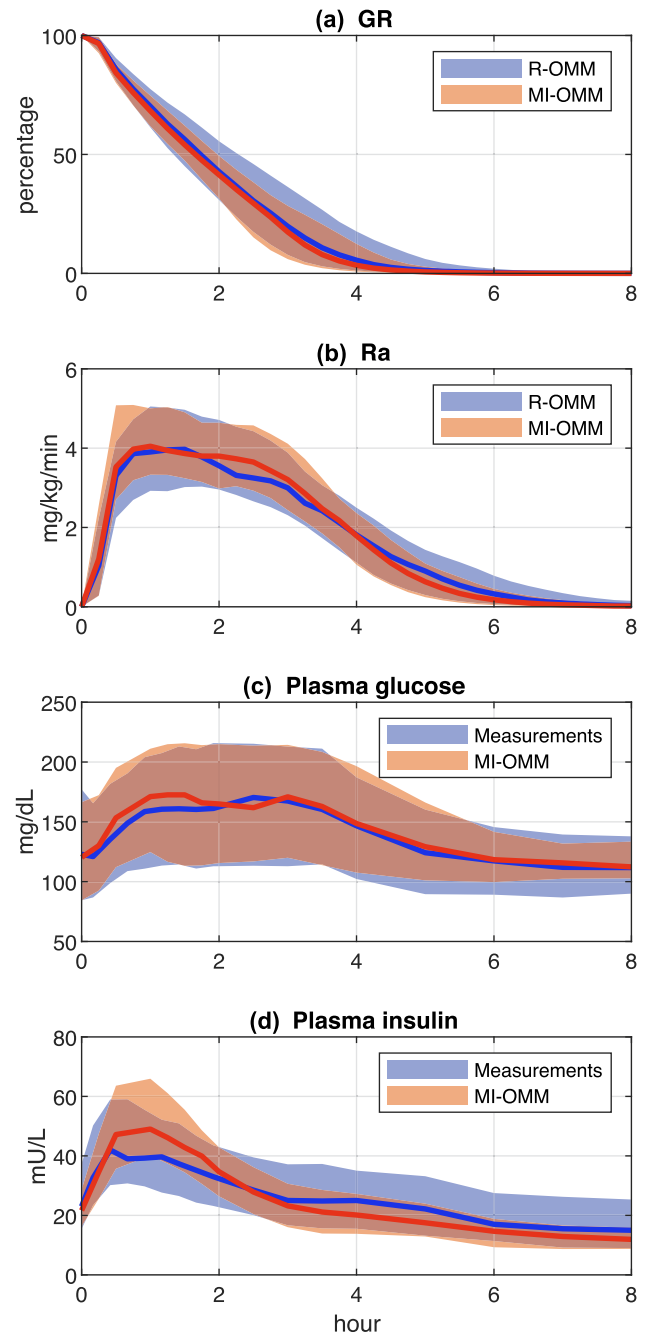

Fig. 6. Comparison of MI-OMM results (red lines and orange areas) against curves obtained with R-OMM and original data (blue lines and light blue areas). Thick lines represent medians, while shaded areas represent 25th and 75th percentile ranges. *Panel A:* GR(t) obtained from R-OMM and MI-OMM. *Panel B:* R_a(t) obtained from R-OMM and MI-OMM. *Panel C:* Measured plasma glucose and G(t) obtained from MI-OMM. *Panel D:* Measured plasma insulin and I_p(t) obtained from MI-OMM.

speculate that the MI-OMM was tested in a challenging scenario, still providing satisfactory results. More recent and accurate glucose sensors are available to researchers and people with diabetes all over the world. We believe that the performance of MI-OMM could greatly improve if the model was fed with the data collected with such devices. Furthermore, with the advent

of real-time insulin sensors [38], [39], [40], the complexity of the MI-OMM could be reduced by eliminating, in part or completely, the insulin subsystem (Section II-C1) and using measurements from the insulin sensors instead. In addition to that, the direct measurement of plasma insulin would allow for the identification of the MI-OMM in subjects with T2D, without the need to extend the already-complex MI-OMM with a sub-model for insulin secretion, which may be a rather challenging task.

As already anticipated, we plan to apply the MI-OMM to the aforementioned dataset containing data of patients with T1D studied in real-life conditions while wearing CGM and IP. The aim will be to detect differences in the GR, R_a and S_I depending on the type of meal, such as high vs low-fat content, or high-fat vs high-protein content. Needless to say, before going to this stage of our research we first needed to develop and validate the MI-OMM in a dataset where plasma glucose and insulin measurements were collected together with CGM and IP data. Future work would also include the analysis of the MI-OMM using nonlinear mixed-effects modeling. Within this framework, we expect to introduce the information about meal composition directly into the model, as a descriptor for model parameters.

Extending the R-OMM, used in hospitalized settings, to the MI-OMM, applicable in real-life scenarios, can really be a game-changer in the treatment of diabetes due to the recently available large amount of data coming from wearable devices, which would allow improving diabetes management while limiting the need of expensive clinical trials and patient's burden. In addition, we believe that our model has the potential to improve diabetes management by understanding the key factors affecting meal absorption and insulin sensitivity in real-life scenarios and consequently adjusting the treatment. This can be potentially used to re-design current insulin therapies, or in more advanced frameworks, the model itself could be incorporated in automatic controllers for insulin delivery or used to inform machine learning techniques for detecting unannounced meals. Finally, upcoming sensors and insulin infusion devices would only improve model performances and extend its range of applicability (e.g., patients with T2D) in the future.

V. Conclusion

In this work, we developed a model for the estimation of GR, R_a, and S_I after a meal, in patients with T1D wearing a CGM sensor and an IP. The presented model is an extension of the OMM, which was previously developed to work with data collected in hospitalized settings. The MI-OMM is able to provide an accurate and physiologically interpretable quantification of those quantities in daily-life conditions as proven by comparison with the R-OMM. GR, R_a, and S_I are known to be strongly affected by meal composition, and for this reason, the next step of our work will be the application of the MI-OMM to a dataset where meals with different compositions were consumed by the patients with T1D, with the objective of detecting how and how much each macronutrient affects GR, R_a, and S_I, and thus also the post-prandial glucose excursion. Thanks to the easily accessible data that it requires, the MI-OMM has potentially multiple

other applications, such as the incorporation into controllers for insulin delivery or algorithms for meal detection. Finally, the employment of such knowledge in open- and closed-loop diabetes therapies would allow a great step ahead toward the optimal insulin dosing in patients with diabetes.

Appendix

A. Initial Conditions and Integration of Model Equations

In real-life conditions, it may happen that the system is not in steady state at the time of the meal. This can lead to the problem of setting the proper initial conditions for model integration. Here below, we reported the strategy implemented in this work to overcome this issue. For what concerns the submodel of the subcutaneous insulin absorption (Section II-C1), it was integrated from the time corresponding to the first available IP rate datum, exploiting the fact that these data were available several hours before the starting of the experiment. Therefore, we could safely identify such time with $-\infty$ and assume that the subsystem was at steady state earlier than this time. The submodels describing glucose-insulin dynamics and the interstitial glucose kinetics (Section II-B, (1), and Section II-C2) were integrated from t=−15 min, assuming $R_a(-15)=0$. Initial conditions were calculated by solving (1) and (5):

$$G_i(-15) = CGM(-15) \tag{11}$$

$$G(-15) = G_i(-15) + \dot{G}_i(-15)\,\tau_G \tag{12}$$

$$X(-15) = \frac{G_b\,p_1 - \dot{G}(-15)}{G(-15)} - p_1 \tag{13}$$

where $\dot{G}_i(-15)$ is the derivative of the CGM measurements at −15 min, calculated by applying a weighted linear regression to CGM data collected between −15 min and 0 min, and $\dot{G}(-15)$ was assumed equal to $\dot{G}_i(-15)$. Conversely, for what concerns the submodel for the gastrointestinal tract (Section II-B, (2)), it was integrated from t=0, with all initial conditions set to zero, assuming the stomach of the patient was empty at that time.

References

[1] American Diabetes Association Professional Practice Committee, "2. Classification and diagnosis of diabetes: Standards of medical care in diabetes—2022," *Diabetes Care*, vol. 45, no. Supplement_1, pp. S17–S38, Jan. 2022.

[2] American Diabetes Association Professional Practice Committee, "12. Retinopathy, neuropathy, and foot care: Standards of medical care in diabetes—2022," *Diabetes Care*, vol. 45, no. Supplement_1, pp. S185–S194, Jan. 2022.

[3] M. Paterson et al., "The role of dietary protein and fat in glycaemic control in type 1 diabetes: Implications for intensive diabetes management," *Curr. Diabetes Rep.*, vol. 15, no. 9, Jul. 2015, Art. no. 61.

[4] K. J. Bell et al., "Impact of fat, protein, and glycemic index on postprandial glucose control in type 1 diabetes: Implications for intensive diabetes management in the continuous glucose monitoring era," *Diabetes Care*, vol. 38, no. 6, pp. 1008–1015, May 2015.

[5] C. E. M. Smart, B. R. King, and P. E. Lopez, "Insulin dosing for fat and protein: Is it time?," *Diabetes Care*, vol. 43, no. 1, pp. 13–15, Dec. 2019.

[6] M. Metwally et al., "Insulin pump dosing strategies for meals varying in fat, protein or glycaemic index or grazing-style meals in type 1 diabetes: A systematic review," *Diabetes Res. Clin. Pract.*, vol. 172, Feb. 2021, Art. no. 108516.

[7] M. Lodefalk, J. Åman, and P. Bang, "Effects of fat supplementation on glycaemic response and gastric emptying in adolescents with type 1 diabetes," *Diabetic Med.*, vol. 25, no. 9, pp. 1030–1035, Aug. 2008.

[8] M. A. Khan, M. C. Gannon, and F. Q. Nuttall, "Glucose appearance rate following protein ingestion in normal subjects," *J. Amer. College Nutr.*, vol. 11, no. 6, pp. 701–706, Dec. 1992.

[9] C. E. M. Smart et al., "Both dietary protein and fat increase postprandial glucose excursions in children with type 1 diabetes, and the effect is additive," *Diabetes Care*, vol. 36, no. 12, pp. 3897–3902, Nov. 2013.

[10] P. Ježek et al., "Fatty acid-stimulated insulin secretion vs. lipotoxicity," *Molecules*, vol. 23, no. 6, Jun. 2018, Art. no. 1483.

[11] K. J. Bell et al., "Optimized mealtime insulin dosing for fat and protein in type 1 diabetes: Application of a model-based approach to derive insulin doses for open-loop diabetes management," *Diabetes Care*, vol. 39, no. 9, pp. 1631–1634, Jul. 2016.

[12] K. J. Bell et al., "Amount and type of dietary fat, postprandial glycemia, and insulin requirements in type 1 diabetes: A randomized within-subject trial," *Diabetes Care*, vol. 43, no. 1, pp. 59–66, Aug. 2019.

[13] C. Dalla Man, M. Camilleri, and C. Cobelli, "A system model of oral glucose absorption: Validation on gold standard data," *IEEE Trans. Biomed. Eng.*, vol. 53, no. 12, pp. 2472–2478, Dec. 2006.

[14] R. Basu et al., "Use of a novel triple-tracer approach to assess postprandial glucose metabolism," *Amer. J. Physiol.- Endocrinol. Metab.*, vol. 284, no. 1, pp. E55–E69, Jan. 2003.

[15] A. Mari et al., "A model-based method for assessing insulin sensitivity from the oral glucose tolerance test," *Diabetes Care*, vol. 24, no. 3, pp. 539–548, Mar. 2001.

[16] C. D. Man, A. Caumo, and C. Cobelli, "The oral glucose minimal model: Estimation of insulin sensitivity from a meal test," *IEEE Trans. Biomed. Eng.*, vol. 49, no. 5, pp. 419–429, May 2002.

[17] M. Schiavon et al., "A new index of insulin sensitivity from glucose sensor and insulin pump data: In silico and in vivo validation in youths with type 1 diabetes," *Diabetes Technol. Therapeutics*, vol. 25, no 4, pp. 270–278, 2023.

[18] J. Hughes et al., "Replay simulations with personalized metabolic model for treatment design and evaluation in type 1 diabetes," *J. Diabetes Sci. Technol.*, vol. 15, no. 6, pp. 1326–1336, Nov. 2020.

[19] G. Cappon et al., "ReplayBG: A digital twin-based methodology to identify a personalized model from type 1 diabetes data and simulate glucose concentrations to assess alternative therapies," *IEEE Trans. Biomed. Eng.*, vol. 70, no. 11, pp. 3227–3238, Nov. 2023.

[20] Y. M. Luijf et al., "Day and night closed-loop control in adults with type 1 diabetes," *Diabetes Care*, vol. 36, no. 12, pp. 3882–3887, Nov. 2013.

[21] A. Mallad et al., "Nocturnal glucose metabolism in type 1 diabetes: A study comparing single versus dual tracer approaches," *Diabetes Technol. Therapeutics*, vol. 17, no. 8, pp. 587–595, Aug. 2015.

[22] M. Schiavon, C. D. Man, and C. Cobelli, "Modeling subcutaneous absorption of fast-acting insulin in type 1 diabetes," *IEEE Trans. Biomed. Eng.*, vol. 65, no. 9, pp. 2079–2086, Sep. 2018.

[23] E. Faggionato et al., "Modeling between-subject variability in subcutaneous absorption of a fast-acting insulin analogue by a nonlinear mixed effects approach," *Metabolites*, vol. 11, no. 4, Apr. 2021, Art. no. 235.

[24] K. Rebrin et al., "Subcutaneous glucose predicts plasma glucose independent of insulin: Implications for continuous monitoring," *Amer. J. Physiol.-Endocrinol. Metab.*, vol. 277, no. 3, pp. E561–E571, Sep. 1999.

[25] M. Schiavon et al., "Quantitative estimation of insulin sensitivity in type 1 diabetic subjects wearing a sensor-augmented insulin pump," *Diabetes Care*, vol. 37, no. 5, pp. 1216–1223, Apr. 2014.

[26] G. Toffolo et al., "A minimal model of insulin secretion and kinetics to assess hepatic insulin extraction," *Amer. J. Physiol.- Endocrinol. Metab.*, vol. 290, no. 1, pp. E169–E176, Jan. 2006.

[27] S. Audoly et al., "Global identifiability of nonlinear models of biological systems," *IEEE Trans. Biomed. Eng.*, vol. 48, no. 1, pp. 55–65, Jan. 2001.

[28] S. E. Kahn et al., "Treatment with a somatostatin analog decreases pancreatic B-cell and whole body sensitivity to glucose," *J. Clin. Endocrinol. Metab.*, vol. 71, no. 4, pp. 994–1002, Oct. 1990.

[29] C. Cobelli and E. Carson, "Parametric models–the estimation problem," in *Introduction to Modeling in Physiology and Medicine*. Amsterdam, The Netherlands: Elsevier, 2008, ch. 8, pp. 195–234.

[30] C. D. Man et al., "Meal simulation model of the glucose-insulin system," *IEEE Trans. Biomed. Eng.*, vol. 54, no. 10, pp. 1740–1749, Oct. 2007.

[31] A. Facchinetti et al., "Modeling the glucose sensor error," *IEEE Trans. Biomed. Eng.*, vol. 61, no. 3, pp. 620–629, Mar. 2014.

[32] G. T. Walker, "On periodicity in series of related terms," *Proc. Roy. Soc. London. Ser. A., Containing Papers Math. Phys. Character*, vol. 131, no. 818, pp. 518–532, Jun. 1931.

[33] The MathWorks Inc., "Documentation of MATLAB, version R2020a," Natick, MA, USA, 2022. Accessed: Mar. 30, 2023. [Online]. Available: https://mathworks.com/help/releases/R2020a

[34] D. Tricò and A. Natali, "Modulation of postprandial glycemic responses by noncarbohydrate nutrients provides novel approaches to the prevention and treatment of type 2 diabetes," *Amer. J. Clin. Nutr.*, vol. 106, no. 2, pp. 701–702, Aug. 2017.

[35] M. Camilleri and A. Shin, "Novel and validated approaches for gastric emptying scintigraphy in patients with suspected gastroparesis," *Dig. Dis. Sci.*, vol. 58, no. 7, pp. 1813–1815, May 2013.

[36] M. Schiavon et al., "Improved postprandial glucose metabolism in type 2 diabetes by the dual glucagon-like peptide-1/glucagon receptor agonist SAR425899 in comparison with liraglutide," *Diabetes, Obesity Metab.*, vol. 23, no. 8, pp. 1795–1805, May 2021.

[37] E. Faggionato et al., "1359-P: Effect of fat content on postprandial gastric retention and glucose absorption in subjects with type 1 diabetes during daily life conditions: Assessment through a computational model," *Diabetes*, vol. 71, no. Supplement_1, Jun. 2022, Art. no. 1359-P.

[38] Z. Hao et al., "Real-time monitoring of insulin using a graphene field-effect transistor aptameric nanosensor," *ACS Appl. Mater. Interfaces*, vol. 9, no. 33, pp. 27504–27511, Aug. 2017.

[39] P. Arpaia et al., "A micro-bioimpedance meter for monitoring insulin bioavailability in personalized diabetes therapy," *Sci. Rep.*, vol. 10, no. 1, Aug. 2020, Art. no. 13656.

[40] E. Vargas et al., "Insulin detection in diabetes mellitus: Challenges and new prospects," *Nature Rev. Endocrinol.*, vol. 19, no. 8, pp. 487–495, May 2023.